JACS
JOURNAL OF THE AMERICAN CHEMICAL SOCIETY

Communication

pubs.acs.org/JACS

Direct Observation of Energy Detrapping in LH1-RC Complex by Two-Dimensional Electronic Spectroscopy

Fei Ma,*[,†] Long-Jiang Yu,[‡,§] Ruud Hendrikx,[†] Zheng-Yu Wang-Otomo,[‡] and Rienk van Grondelle[†]

[†]Department of Biophysics, Faculty of Sciences, VU University Amsterdam, De Boelelaan 1081, 1081 HV Amsterdam, The Netherlands

[‡]Faculty of Science, Ibaraki University, Mito, Ibaraki 310-8512, Japan

[§]Research Institute for Interdisciplinary, Okayama University, Tsushima Naka 3-1-1, Okayama 700-8530, Japan

Supporting Information

ABSTRACT: The purple bacterial core light harvesting antenna-reaction center (LH1-RC) complex is the simplest system able to achieve the entire primary function of photosynthesis. During the past decade, a variety of photosynthetic proteins were studied by a powerful technique, two-dimensional electronic spectroscopy (2DES). However, little attention has been paid to LH1-RC, although its reversible uphill energy transfer, trapping, and backward detrapping processes, represent a crucial step in the early photosynthetic reaction dynamics. Thus, in this work, we employed 2DES to study two LH1-RC complexes of *Thermochromatium* (*Tch.*) *tepidum*. By direct observation of detrapping, the complex reversible process was clearly identified and an overall scheme of the excitation evolution in LH1-RC was obtained.

Photosynthesis powers the biosphere by harvesting sunlight to separate electrical charge, as a result converting solar into chemical energy. The simplest photosynthetic organism to achieve this function is a purple bacterial reaction center (RC) enclosed by a core light-harvesting antenna (LH1), referred to as the LH1-RC complex. Recent crystal structures show that in the purple bacterium *Thermochromatium* (*Tch.*) *tepidum*, LH1 is a closed elliptical ring containing 16 heterodimers of $\alpha\beta$-subunit and 32 bacteriochlorophyll (BChl) *a* molecules sandwiched between the rings of α and β polypeptides (Figure 1A).[1,2] Excitation on LH1 is trapped by a special pair of BChl *a* (P) in the RC, an uphill process with a rate (k_t) of (30−65 ps)$^{-1}$.[3−10] From P*, primary charge separation occurs whereby an electron is transferred to a monomeric BChl *a* (B) with a rate (k_c) of (3−5 ps)$^{-1}$, followed by formation of the P^+B^- charge-transfer state.[11] At the same time, the opposite process to trapping, backward energy transfer (EET) from P* to LH1 (detrapping) with a rate (k_{-t}) of (4−25 ps)$^{-1}$,[4−6,12−14] competes with charge separation. This back-transfer process is important as it ultimately determines the efficiency of excitation energy utilization.

The LH1-RC of *Tch. tepidum* is an excellent system to investigate these processes, due to the different spectral forms it can form. In native LH1, a Ca^{2+} binds at the C-terminal of each $\alpha\beta$-subunit and connects the α and β chains.[1] The lowest excited-state (Q_y) absorption of BChl *a* is peaked at 915 nm (Figure S1), significantly redder than most LH 1s of other purple bacteria. The spectral form of LH1 can be modified by substituting Ca^{2+} with Ba^{2+}, in which Ba^{2+} binds only α chain (Figure 1A).[2] It leads to an inhomogeneity of site energy between the α- and β-BChl *a*. So, the Q_y absorption is blue-shifted to 893 nm.[15,16] In both Ca-LH1-RC and Ba-LH1-RC, the structures of RC are nearly identical and the absorption of P peaks at 890 nm.[1,2,10] At 77 K, the absorptions of Ca-LH1, Ba-LH1 and P peak at 935 (B935), 910 (B910) and 910 nm, respectively (Figure 1B). These unique complexes, with the donor energy level varied while the other factors (energy level of acceptor, orientation factor) remaining almost the same, provide a natural model to quantitatively investigate excitation uphill transfer and back-transfer processes.

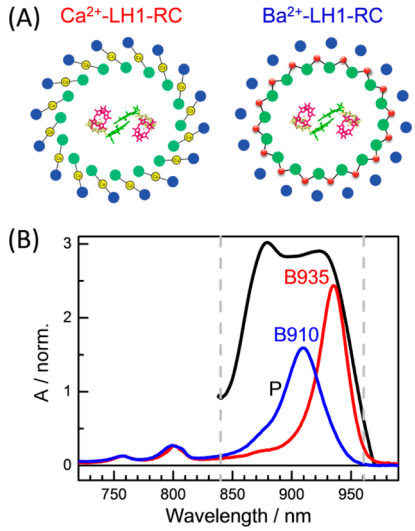

Figure 1. (A) Supramolecular architecture of the two LH1-RC complexes of *Tch. tepidum*.[2] Display strategy: dark green (dark blue) ball, α- (β-)polypeptide; yellow (red) balls, Ca^{2+} (Ba^{2+}); green, P; pink, B. (B) 77 K linear absorption spectra of Ca-LH1-RC (red) and Ba-LH1-RC (blue), normalized with regard to the carotenoid absorption bands at 550 nm. The spectrum of the excitation pulse is shown in black and the detection range in the experiment is limited within the gray dashed lines.

Energy and charge transfer dynamics in LH1-RC were studied extensively with transient absorption and fluorescence (FL) spectroscopy.[3−6,12−14,17] Our earlier transient absorption

Received: October 26, 2016
Published: December 22, 2016

DOI: 10.1021/jacs.6b11017
J. Am. Chem. Soc. 2017, 139, 591−594

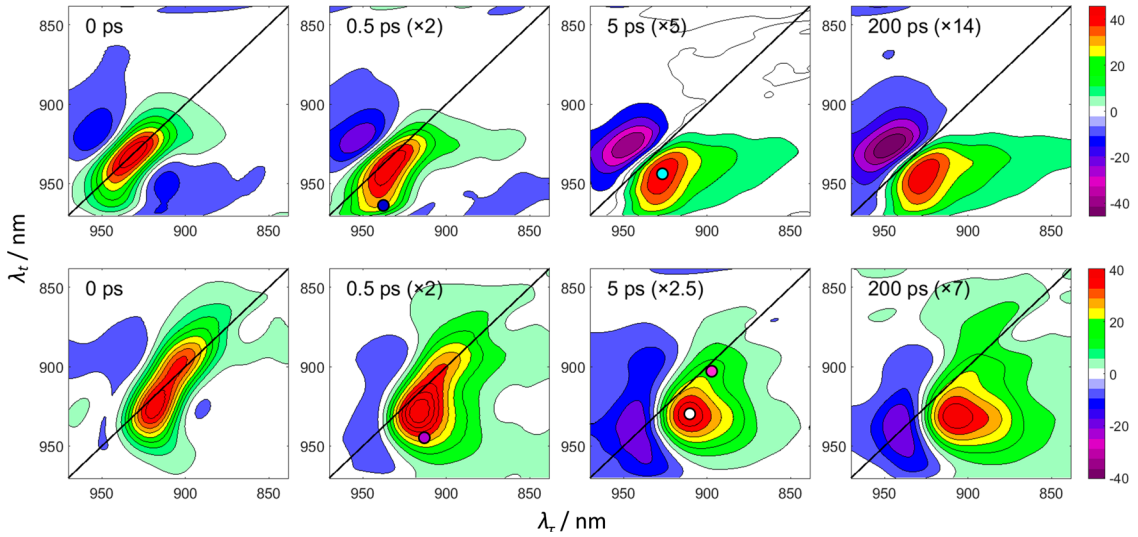

Figure 2. 77 K 2D real rephasing spectra of Ca-LH1-RC (top) and Ba-LH1-RC (bottom) at the indicated population times (T). λ_τ and λ_t are excitation and detection wavelengths, respectively. The colored circles correspond to the cross peaks.

measurement has determined k_t to be $(65\ \text{ps})^{-1}/(225\ \text{ps})^{-1}$ and $(58\ \text{ps})^{-1}/(45\ \text{ps})^{-1}$ for Ca-LH1-RC and Ba-LH1-RC, respectively, at room temperature (RT)/77 K.[10] However, the detrapping process was not unambiguously identified, although a 2−3 ps decay component observed (Figure S2) could be attributable to detrapping.[12−14]

In this work, we employed two-dimensional electronic spectroscopy (2DES)[18−20] to investigate the excitation evolution dynamics in the two LH1-RC complexes. 2DES provides full correlation maps between excitation and probing wavelengths and thus can obtain the full connectivity network between electronic transitions. Hence it is advantageous, as displayed in this work, in (i) directly tracking EET dynamics, due to appearance of corresponding signals as cross peaks; (ii) unraveling inhomogeneity of a band, which is usually hidden in the case of one-dimensional time-resolved methods. Hence 2DES was successfully applied in studies of various photosynthetic proteins.[21−27] And this work, to the best of our knowledge, constitutes the first 2DES study of the LH ⇌ RC EET, the last step of the overall EET process in purple bacteria.

The 2D real rephasing spectra of the two complexes exhibit clear differences (Figure 2), which appear immediately upon excitation. At T = 0, the spectrum of Ca-LH1-RC contains a positive ground state bleach (GSB) signal symmetric along the diagonal, a spectral shape conserved among other antenna complexes.[24−26] But for Ba-LH1-RC, the GSB signal of B910 contains two bands, peaked at (918, 923) and (904, 899) nm. The same behavior also appears in the nonrephasing spectra (see Figures S3 and S4). It is in line with the 77 K FL spectrum showing a band splitting with an energy difference of 550 cm^{-1} (Figure 4). The band splitting indicates that B910 contains two "pools" of BChls *a*. It should origin from the structural property that Ba^{2+}-bound α-BChl is energetically lower than the unbound β-BChl.[2] So, the (918, 923) and (904, 899) nm peaks are attributed to lower- and higher energy BChl *a*, respectively. Our 2DES discloses this feature, which was not revealed previously by transient absorption measurement.[10] The long axis of the B910 GSB signals slightly deviates from the diagonal, it could be the result of an inhomogeneous superposition of the negative excited state absorption (ESA) signals belonging to the two sets of BChl *a*. This is implied from the spectra at longer T, where the ESA is above the diagonal for shorter λ_τ whereas crosses the diagonal for longer λ_τ.

Fast decoherence takes place in ∼50 fs.[24−26] Within this process, excitation transfers among several exciton states and a new excited-state equilibrium in the exciton manifold is built up. This can be seen from the appearance of a cross peak at (935, 965) nm for Ca-LH1-RC and (910, 945) nm for Ba-LH1-RC (blue and purple curcles in the T = 0.5 ps spectra in Figure 2), representing the population of the lowest exciton state.

Within 1−3 ps, a new cross peak(s) becomes more dominant (T = 5 ps spectra in Figure 2). It is superimposed with GSB signal. In Ca-LH1-RC, the observed peak is at (930, 945) nm (light blue circle). Although deviated from (910, 935) nm, the feature of this positive band reflects EET from P* to B935. Thus, the detrapping process can be identified. In Ba-LH1-RC, the main cross peak is at (910, 935) nm (white circle). Further, there is another weaker cross peak, indicated by its extension at (898, 904) nm (pink circle). The two peaks correspond to the energy detrapping from P* to the lower-energy-B910 and higher-energy-B910, respectively.

It is notable that the detrapping cross peaks spread to wavelengths as short as 850 nm. Furthermore, it is structured, containing a minor peak at λ_τ = 895 nm. These features may imply that excitation on both P_A and P_B can be detrapped by LH1. It is also possible that the minor peak is associated with the P^+B^- charge-transfer state.

Then the GSB and the cross peak decay synchronously (T = 200 ps spectra in Figure 2), attributed to LH1→P trapping. The fact that the cross peak decays with the depopulation of LH1 supports its backward energy-transfer nature. A corresponding cross peak is supposed to appear at, for example, (935, 910) nm for Ca-LH1-RC; however, it is not observed due to superposition of the relatively strong ESA.

One thing to be noted is the possibility that the dynamics of the two split B910 bands are different. The two sets of BChl *a* with different energies may exhibit different trapping and detrapping rates. However, no clear difference can be identified beyond the error level, regarding the time constants of the GSB recovery and of the cross peak formation and decay. This is most probably the result of ultrafast coherent exciton migration among α- and β-BChl *a*. As previously studied, the delocalization length

DOI: 10.1021/jacs.6b11017
J. Am. Chem. Soc. 2017, 139, 591−594

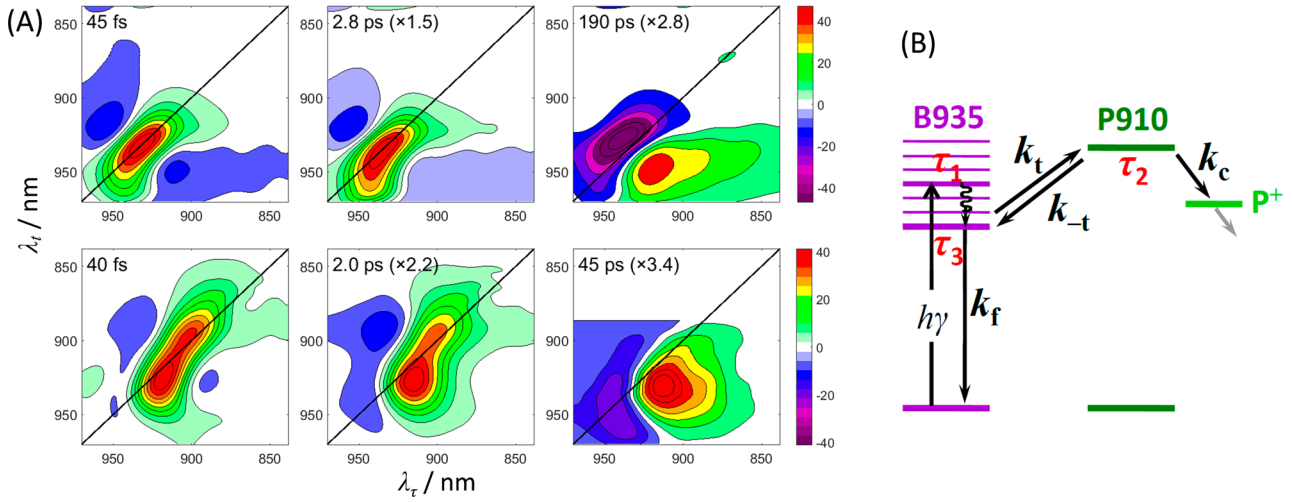

Figure 3. (A) 77 K 2D decay-associated spectra of Ca-LH1-RC (top) and Ba-LH1-RC (bottom). (B) Scheme of EET and primary charge separation processes in Ca-LH1-RC.

Table 1. Decay Time Constants Obtained by 2D Global DAS Analysis of Ca-LH1-RC and Ba-LH1-RC, Trapping and Detrapping Rates, and Relative Spectral Overlap Integrate for Trapping (A_t) and Detrapping (A_{-t})

	77 K							Room temperature						
	τ_1 (fs)	τ_2 (ps)	τ_3 (ps)	k_t^{-1}[a]	k_{-t}^{-1}[b]	A_t	A_{-t}	τ_1 (fs)	τ_2 (ps)	τ_3 (ps)	k_t^{-1}	k_{-t}^{-1}	A_t	A_{-t}
Ca^{2+}-LH1-RC	45	2.8	190	235	9.3	1.0[c]	7.5	50	2.0	65	70	4.0	3.3	11.7
Ba^{2+}-LH1-RC	40	2.0	45	47	4.0	5.0	9.8	50	1.4	60	64	2.2	5.1	12.6

[a]Unit of k_t and k_{-t}: ps^{-1}. [b]k_{-t} is an estimated value from $\tau_2 = (k_{-t} + k_c)^{-1}$ and $k_c = (4\ ps)^{-1}$. [c]A_t and A_{-t} were normalized with regard to this value.

is 2−4 BChl molecules in LH1.[28] So, for further global analysis, we treat the two sets as one nondistinguishable generated state.

Global analysis with a sequential model provides characteristic time constants of dynamic processes without assuming an exact model. The 2D decay associated spectra (DAS) of three exponentially decay components are shown in Figure 3A, with time constants (τ_1, τ_2 and τ_3 in Table 1) of 45/40 fs, 2.8/2.0 ps and 190/45 ps for Ca-LH1-RC/Ba-LH1-RC, respectively. The first component represents the initial exciton manifold upon excitation, which evolves into a new equilibrium promptly. It is notable that τ_1 is only a little dependent on temperature, 45/40 fs at 77 K and 50/50 fs at RT (Figures S5 and S6 for the RT 2DES and DAS spectra); and is nearly independent of the subtle structural difference between Ca-LH1 and Ba-LH1.

The second component is characteristic of the broadened GSB band and the appearance of a cross peak corresponding to EET from higher to the lowest exciton state. τ_2 is the time constant for the formation of the cross peak corresponding to P*→LH1 detrapping and is dependent on both sample and temperature, 2.8/2.0 ps at 77 K and 2.0/1.4 ps at RT. Thus, it is attributed to the lifetime of P*. The third component contains predominantly the ESA of LH1-Q_y and the detrapping cross peak, whose decay reflects the recovery of the LH1-Q_y ground state. So, τ_3 represents the lifetime of LH1. It is sensitive to the sample and temperature, 190/45 ps at 77 K and 65/60 ps at RT. The values of τ_3 are in agreement with our previous transient absorption results.[10]

The dynamic scheme for the Ca-LH1-RC is described in Figure 3B. Accordingly, $\tau_3 = (k_t + k_f)^{-1}$, k_f ($(\sim 1\ ns)^{-1}$) is much smaller than k_t. Thus, the trapping rate k_t is close to τ_3^{-1}. However, the detrapping rate k_{-t} cannot be determined directly from $\tau_2 = (k_{-t} + k_c)^{-1}$, because the values of k_{-t} and k_c are in the same level. k_c is normally determined in isolated RCs after direct excitation of P.[11] We assume $k_c = (4\ ps)^{-1}$ for all the cases, as a result, k_{-t} is estimated to be 9.3/4.0 ps at 77 K and 4.0/2.2 ps at RT for Ca-/Ba-LH1-RC, respectively.

The distances between LH1 and P are 37.4−49.0 Å,[1,2] so trapping and detrapping should obey Förster's hopping mechanism.[27] According to Förster theory, the EET rate is proportional to the spectral overlap integral, $J_F = \int_0^\infty \overline{f}_D(\lambda)\varepsilon_A(\lambda)\lambda^4\, d\lambda$, where $\overline{f}_D(\lambda)$ is the normalized FL spectrum of donor, $\varepsilon_A(\lambda)$ is the absorption spectrum of acceptor. Our 2DES results show that both k_t and k_{-t} are smaller in Ca-LH1-RC than those in Ba-LH1-RC. We compared the spectral overlap integrals J_F (Figure 4 and Table 1) to understand the difference. At 77 K, the FL of Ba-LH1-RC contains two bands, attributable to the lower- and higher energy sets of BChl *a*. Population of the higher-energy band increases the trapping efficiency. The 77 K FL spectrum of Ca-LH1 also contains a minor higher-energy band. It may be because that a small portion of Ca^{2+}-binding is missing, inducing a population of the higher-energy band. The ratio of J_F between Ca-LH1-RC and Ba-LH1-RC is 0.21 at 77 K and 0.66 at RT. These calculations well explain the fact that at low temperature, trapping is much less efficient in Ca-LH1-RC. An explicit calculation of k_t is shown in SI. For detrapping, the J_F of Ca-LH1-RC is also smaller than that of Ba-LH1-RC, the relative ratio being 0.75 at 77 K and 0.92 at RT. The values can qualitatively explain the smaller k_{-t} in Ca-LH1-RC.

At last, we compare the efficiencies of the two key processes between the two complexes: LH1→RC EET (Φ_{ET}) determined by $k_t/(k_t + k_f)$ and primary charge separation (Φ_{CT}) determined by $k_c/(k_{-t} + k_c)$. Because k_f is much smaller than k_t, decrease of k_t from $(45\ ps)^{-1}$ to $(190\ ps)^{-1}$ only decreases Φ_{ET} from 0.96 to 0.84 at 77 K. At RT, the difference, 0.96 for Ba-LH1-RC and 0.94 for Ca-LH1-RC, is nearly negligible. Φ_{CT} is more sensitive to k_{-t},

DOI: 10.1021/jacs.6b11017
J. Am. Chem. Soc. 2017, 139, 591−594

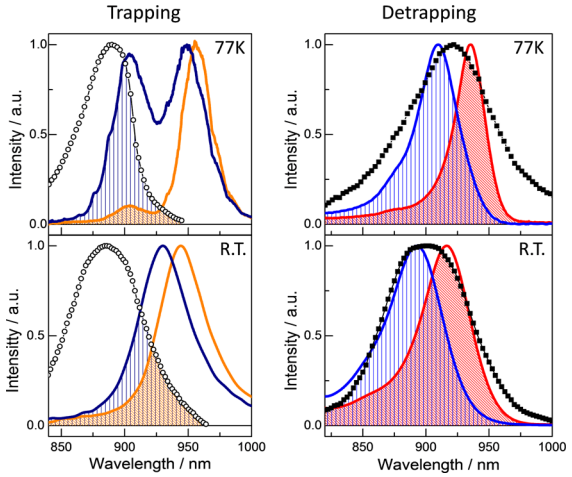

Figure 4. Comparison of Förster spectral overlap for trapping (left) and detrapping (right) at 77 K (top) and RT (bottom). Orange (dark blue) lines represent the f_D of Ca-LH1(Ba-LH1); red (blue) lines the ε_A of Ca-LH1 (Ba-LH1); open circles (closed square) the ε_A (f_D) of P.

a decrease of k_{-t} from $(2.2\ \text{ps})^{-1}$ to $(4.0\ \text{ps})^{-1}$ and to $(9.3\ \text{ps})^{-1}$ increases Φ_{CT} from 0.35, 0.50 to 0.70. So, primary charge separation is more beneficial in Ca-LH1-RC. In summary, a red-shift of LH1-Q_y results in a slightly decreased Φ_{ET} and a considerably increased Φ_{CT}. The influences of metal cations binding on structure and physiological function are discussed in the SI.

The two LH1-RC complexes of *Tch. tepidum* provide an excellent system to investigate the influence of pigment supramolecular structure on the electronic properties and consequently on the effective processes of light-induced photosynthetic EET and charge separation. With 2DES spectroscopy, the detrapping was directly identified and we obtained an overall scheme of the dynamic processes. The trapping and detrapping rates were quasi-quantitatively analyzed with Förster spectral overlap. Further, we revealed a spectral splitting in Ba-LH1-RC, consistent with the recently reported crystal structure.

■ ASSOCIATED CONTENT

Supporting Information

The Supporting Information is available free of charge on the ACS Publications website at DOI: 10.1021/jacs.6b11017.

Experimental methods, transient absorption dynamics, nonrephasing 2DES spectra at 77 K, rephrasing 2DES spectra and DAS at RT, k_t calculation and significance of metal cations binding (PDF)

■ AUTHOR INFORMATION

Corresponding Author

*fma@iccas.ac.cn

ORCID

Fei Ma: 0000-0002-7607-6429

Notes

The authors declare no competing financial interest.

■ ACKNOWLEDGMENTS

We thank the group of professor Bruno Robert, CEA Saclay, France for the low-temperature fluorescence measurements. F.M. and R.v.G. were supported by an Advanced Investigator grant from the European Research Council (No. 267333, PHOTPROT) to R.v.G and the TOP-grant (700.58.305) from the Foundation of Chemical Science part of NOW. R.v.G. gratefully acknowledges his Academy Professor grant from The Netherlands Royal Academy of Sciences (KNAW).

■ REFERENCES

(1) Niwa, S.; Yu, L.-J.; Takeda, K.; Hirano, Y.; Kawakami, T.; Wang-Otomo, Z.-Y.; Miki, K. *Nature* **2014**, *508*, 228.
(2) Yu, L.-J.; Kawakami, T.; Kimura, Y.; Wang-Otomo, Z.-Y. *Biochemistry* **2016**, *55*, 6495.
(3) Visscher, K. J.; Bergström, H.; Sundström, V.; Hunter, C. N.; van Grondelle, R. *Photosynth. Res.* **1989**, *22*, 211.
(4) Timpmann, K.; Freiberg, A.; Sundström, V. *Chem. Phys.* **1995**, *194*, 275.
(5) Freiberg, A.; Allen, J. P.; Williams, J. C.; Woodbury, N. W. *Photosynth. Res.* **1996**, *48*, 309.
(6) Bernhardt, K.; Trissl, H.-W. *Biochim. Biophys. Acta, Bioenerg.* **2000**, *1457*, 1.
(7) Sundström, V.; Pullerits, T.; van Grondelle, R. *J. Phys. Chem. B* **1999**, *103*, 2327.
(8) Yang, M.; Agarwal, R.; Fleming, G. R. *J. Photochem. Photobiol., A* **2001**, *142*, 107.
(9) Cogdell, R. J.; Gardiner, A. T.; Roszak, A. W.; Law, C. L.; Southall, J.; Isaacs, N. W. *Photosynth. Res.* **2004**, *81*, 207.
(10) Ma, F.; Yu, L.-J.; Wang-Otomo, Z.-Y.; van Grondelle, R. *Biochim. Biophys. Acta, Bioenerg.* **2016**, *1857*, 408.
(11) van Brederode, M. E.; van Mourik, F.; van Stokkum, I. H. M.; Jones, M. R.; van Grondelle, R. *Proc. Natl. Acad. Sci. U. S. A.* **1999**, *96*, 2054.
(12) Timpmann, K.; Zhang, F.-G.; Freiberg, A.; Sundström, V. *Biochim. Biophys. Acta, Bioenerg.* **1993**, *1183*, 185.
(13) Beekman, L. M. P.; van Mourik, F.; Jones, M. R.; Visser, M.; Hunter, C. N.; van Grondelle, R. *Biochemistry* **1994**, *33*, 3143.
(14) Xiao, W.-Z.; Lin, S.; Taguchi, A. K. W; Woodbury, N. W. *Biochemistry* **1994**, *33*, 8313.
(15) Kimura, Y.; Inada, Y.; Numata, T.; Arikawa, T.; Li, Y.; Zhang, J.-P.; Wang, Z.-Y.; Ohno, T. *Biochim. Biophys. Acta, Bioenerg.* **2012**, *1817*, 1022.
(16) Ma, F.; Yu, L.-J.; Wang-Otomo, Z.-Y.; van Grondelle, R. *Biochim. Biophys. Acta, Bioenerg.* **2015**, *1847*, 1479.
(17) Katiliene, Z.; Katilius, E.; Woodbury, N. W. *Biophys. J.* **2003**, *84*, 3240.
(18) Brixner, T.; Mančal, T.; Stiopkin, I. V.; Fleming, G. R. *J. Chem. Phys.* **2004**, *121*, 4221.
(19) Nuernberger, P.; Ruetzel, S.; Brixner, T. *Angew. Chem., Int. Ed.* **2015**, *54*, 11368.
(20) Dostál, J.; Pšenčík, J.; Zigmantas, D. *Nat. Chem.* **2016**, *8*, 705.
(21) Brixner, T.; Stenger, J.; Vaswani, H. M.; Cho, M.-H.; Blankenship, R. E.; Fleming, G. R. *Nature* **2005**, *434*, 625.
(22) Schlau-Cohen, G. S.; Ishizaki, A.; Calhoun, T. R.; Ginsberg, N. S.; Ballottari, M.; Bassi, R.; Fleming, G. R. *Nat. Chem.* **2012**, *4*, 389.
(23) Chenu, A.; Scholes, G. D. *Annu. Rev. Phys. Chem.* **2015**, *66*, 69.
(24) Ferretti, M.; Novoderezhkin, V. I.; Romero, E.; Augulis, R.; Pandit, A.; Zigmantas, D.; van Grondelle, R. *Phys. Chem. Chem. Phys.* **2014**, *16*, 9930.
(25) Ferretti, M.; Hendrikx, R.; Romero, E.; Southall, J.; Cogdell, R. J.; Novoderezhkin, V. I.; Scholes, G. D.; van Grondelle, R. *Sci. Rep.* **2016**, *6*, 20834.
(26) Dostál, J.; Mancăl, T.; Augulis, R.; Vácha, F.; Pšenčík, J.; Zigmantas, D. *J. Am. Chem. Soc.* **2012**, *134*, 11611.
(27) Mirkovic, T.; Ostroumov, E. E.; Anna, J. M.; van Grondelle, R.; Govindjee; Scholes, G. D. *Chem. Rev.* **2016**, DOI: 10.1021/acs.chemrev.6b00002.
(28) Novoderezhkin, V. I.; Monshouwer, R.; van Grondelle, R. *Biophys. J.* **1999**, *77*, 666.

DOI: 10.1021/jacs.6b11017
J. Am. Chem. Soc. 2017, 139, 591−594